Combining two antitubercular drugs, clofazimine and 4-aminosalicylic acid, in order to improve clofazimine aqueous solubility and 4-aminosalicylic acid thermal stability

Bodart, Laurie; Derlet, Amélie; Buol, Xavier; Leyssens, Tom; Tumanov, Nikolay; Wouters, Johan

Published in:
Journal of Pharmaceutical Sciences

DOI:
10.1016/j.xphs.2020.09.024

Publication date:
2020

Document Version
Peer reviewed version

Combining two antitubercular drugs, clofazimine and 4-aminosalicylic acid, in order to improve clofazimine aqueous solubility and 4-aminosalicylic acid thermal stability

Laurie Bodart[1,*], Amélie Derlet[1], Xavier Buol[2], Tom Leyssens[2], Nikolay Tumanov[1], Johan Wouters[1,*]

[1]Namur Medicine and Drug Innovation Center - Namur Research Institute for LIfe Science (NAMEDIC-NARILIS), Namur Institute of Structured Matter (NISM), Department of Chemistry, University of Namur (UNamur), 61 Rue de Bruxelles, 5000 Namur, Belgium. [2]Institute of Condensed Matter and Nanosciences, UCLouvain, 1 Place Louis Pasteur, B-1348 Louvain-la-Neuve, Belgium.

*** Correspondence to:** Bodart Laurie (Telephone: +32(0)81724569) and Johan Wouters (Telephone: +32(0)81724550) **email addresses:** laurie.bodart@unamur.be (L. Bodart), johan.wouters@unamur.be (J. Wouters).

Abstract: Four forms of a salt combining two antitubercular drugs, clofazimine and 4-aminosalicylic acid, are reported and the crystal structure of two of these forms are described. TG/DSC analysis of all four forms demonstrate an increase in the temperature at which degradation (upon decarboxylation) occurs in comparison to pure 4-aminosalicylic acid. Water solubility evaluation indicates a significant increase of the amount of clofazimine detected in water (10.26 ± 0.52 µg/mL for form I, 12.27 ± 0.32 µg/mL for form II, 7.15 ± 0.43 µg/mL for form III and 8.50 ± 1.24 µg/mL for form IV) in comparison to pure clofazimine (0.20 ± 0.03 µg/mL).

Keywords: clofazimine, 4-aminosalicylic acid, salts, solid-state, polymorph, differential scanning calorimetry, thermogravimetric analysis, solubility.

Introduction

Tuberculosis (TB)[1] is an infectious disease caused by *Mycobacterium tuberculosis* (*M.tb*) which is still among the top causes of death worldwide[1]. Even if drug susceptible tuberculosis is curable with a two months treatment comprising four first-line antibiotics (rifampicin, isoniazid, pyrazinamide and ethambutol) followed by four months continuation phase with isoniazid and rifampicin[2], multidrug resistant (MDR) and extensively drug resistant (XDR) strains of *M. tb* have emerged because of bad compliance or inappropriate use of antitubercular drugs.

In this context, N,5-bis(4-chlorophenyl)-3-propan-2-yliminophenazin-2-amine (clofazimine, CFZ, Fig. 1a), an antimicrobial and anti-inflammatory agent has been selected to be part of the shortened Bangladesh regimen against MDR tuberculosis[3,4]. Clofazimine is also recommended by the World Health Organization (WHO) as a group B agent for the treatment of MDR and XDR tuberculosis[5]. Belonging to the Biopharmaceuticals Classification System class II (BCS II), clofazimine bioavailability is however limited by its low aqueous solubility (<0.001 mg/L [6,7]). Several strategies have been adopted to improve clofazimine solubility e.g. the preparation of inclusion complexes with cyclodextrins or cucurbit[7]uril[8–10], of nanoparticules or nanosuspensions[11,12], of amorphous solid dispersion[13] or the co-administration with lipid vehicles[14]. Another alternative is to take advantage of the basicity of CFZ to prepare salts[15–18].

According to the WHO, 4-amino-2-hydroxybenzoic acid (4-aminosalicylic acid, PAS, Fig. 1b) is classified as a group C drug for the treatment of multidrug resistant tuberculosis[5]. This compound is a prodrug mimicking 4-aminobenzoic acid, the substrate of dihydropteroate synthase[19]. PAS is a BCS III[20] compound with a reported aqueous solubility of 3.22 g/L at 30 °C[6]. It is however known to be unstable at low pH as it can decarboxylate to 3-aminophenol[21] through the formation of the PAS zwitterion (isoelectric point of 2.71)[21]. In the solid-state, the crystalline powder can also decompose under exposition to moisture or heat[22,23]. The

[1] **Abbreviations:** TB: tuberculosis, *M.tb*: *Mycobacterium tuberculosis*, MDR: multi drug resistant, XDR: extensively drug resistant, CFZ: clofazimine, PAS: 4-aminosalicylic acid, GI: gastro-intestinal, FaSSIF/FeSSIF/FaSSGF: Fasted-state simulated intestinal fluid/ Fed-state simulated intestinal fluid/ Fasted-state simulated gastric fluid, LAG: liquid-assisted grinding, DVS: dynamic vapour sorption.

This article contains supplementary material available from the authors by request or via the internet. Available supplementary materials: Comment on the selection of solvents. Tables of experimental details and of hydrogen bond parameters; observed, calculated and difference pattern from structure solution of $CFZNH^+$-PAS^- form II; description of $CFZNH^+$-PAS^--MeCN solvate; variable temperature PXRD patterns, PXRD patterns of the crystalline phase recovered after TG/DSC analysis; typical HPLC chromatograms.

sodium and calcium salts of PAS are however reported to be more stable than the free acid[24]. Moreover PAS salts have also been reported to reduce the gastro-intestinal (GI) side effects associated to PAS[25,26]. More recently, gastro-resistant caps avoiding PAS exposition to the gastric acidic medium and aiming at further diminishing these GI effects have been commercialized[26].

The association of CFZ and PAS is reported for the treatment of XDR-TB[27,28]. Zhang *et al*.[29] have further shown that PAS enhanced CFZ activity *in vitro* and Lu *et al*.[30] have even shown a synergistic effect between both drugs. Similarly, an alternative formulation consisting of salts combining CFZ with PAS could potentially improve clofazimine solubility and PAS stability. The present study reports on the preparation of $CFZNH^+$-PAS^- salts that were characterized in terms of thermal stability and aqueous solubility.

Materials and Methods

Materials

Clofazimine and 4-aminosalicylic acid were purchased from TCI Europe and Sigma Aldrich respectively. Acetonitrile, ethanol and ethyl acetate were used without further purification as crystallization solvents. FaSSIF/FeSSIF/FaSSGF powder was purchased from Biorelevant (London, UK).

Salts preparation

Clofaziminium - 4-aminosalicylate (form I, II and III) were prepared by liquid-assisted grinding (LAG) of equimolar amount of CFZ (75.0 mg, 0.158 mmol) and PAS (24.3 mg, 0.158 mmol) in presence of 30 µL of MeCN (CFZ/PAS 1/1 LAG MeCN) (form I obtained after drying the powder), EtOH (CFZ/PAS 1/1 LAG EtOH, form II) or EtOAc (CFZ/PAS 1/1 LAG EtOAc form III). See the ESI for comment about the choice of the solvents. Grinding experiments were performed in 2 mL Eppendorf tubes®, filled with seven stainless steel balls of 1 mm diameter and one ball of 3 mm diameter. Ball milling was performed for 90 minutes at 30 Hz using a Retsch Mixer Mill 400 apparatus and samples were homogenized every 30 minutes. Single-crystals were obtained by recrystallization, at room temperature (293-298 K), of the CFZ/PAS 1 :1 ground product with MeCN (CFZ/PAS 1/1 LAG MeCN) in a mixture of MeCN and MeOH (for form I) or in MeCN (for $CFZNH^+$-PAS^--MeCN (1:1:1) solvate). Form IV is obtained by slurrying equimolar amount of CFZ (75.0 mg, 0.158 mmol) and PAS (24.3 mg, 0.158 mmol) in water (powder was recovered by centrifugation and then oven-dried at 60°C for one night).

Single-crystal X-ray diffraction (SCXRD)

SCXRD data were collected with an Oxford Diffraction Gemini Ultra R equipped with a Ruby CCD detector. Full data sets were collected with Cu Kα (λ = 1.54184 Å) radiation at 295 and 100 K for form I and at 100 K for $CFZNH^+$-PAS^--MeCN (1:1:1) solvate. Analytical numeric absorption correction (using a multifaceted crystal model based on expressions derived by R.C. Clark & J.S. Reid[31]), followed by empirical absorption correction (using spherical harmonics, implemented in SCALE3 ABSPACK scaling algorithm) were performed within *CrysAlis PRO*[32]. Structure was solved by the dual-space method implemented by *SHELXT*[33] within *Olex2*[34]*.* Refinement by the least-square method implemented by *SHELXL*[35] was performed within *ShelXle*[36]. Non hydrogen atoms were refined anisotropically while hydrogen atoms were refined as riding atoms with isotropic displacement parameter set to 1.2 times that of the parent atom (1.5 times for methyl and OH groups). In the structures determined at 100 K, hydrogen atoms implied in strong H-bonds were located in Fourier map and refined (except for H atoms of PAS^- in the structure of form I because this anion is disordered over three positions). Structure visualization was performed within *Mercury*[37].

High-resolution powder X-ray diffraction and structure solution.

High-resolution PXRD pattern of form II was collected at 295 K in transmission mode with a STOE MP diffractometer (Cu $K\alpha_1$ radiation, λ = 1.54059 Å) between 4 and 40° 2θ angle, with a step size of 0.15°. Sample was filled in a 0.7 mm diameter thin-wall glass capillary. Indexation was performed within F.O.X version 2017.2 [38]. Intensities were extracted by the Le Bail method implemented within F.O.X. and structure solution was performed by a direct-space method within the same program using clofaziminium and 4-aminosalicylate geometries extracted from SCXRD data. Structure was refined within TOPAS V6 [39], using rigid body approach.

PXRD data were collected with the same diffractometer in transmission mode (transmission scan mode) from 4 to 40° 2θ angle after solubility and slurry experiments.

Powder X-ray diffraction (PXRD)

PXRD data were collected with a PANalytical X'PERT PRO Bragg-Brentano diffractometer, using Cu Kα (λ = 1.54184 Å) radiation (2θ angle ranging from 4 to 40° with a step size of 0.0167°).

Variable-temperature PXRD data were collected at 25°C, from 30 to 150°C (data collected every 10°C), at 175 and 200°C with the same diffractometer equipped with an Anton-Paar TTK 450 heating system.

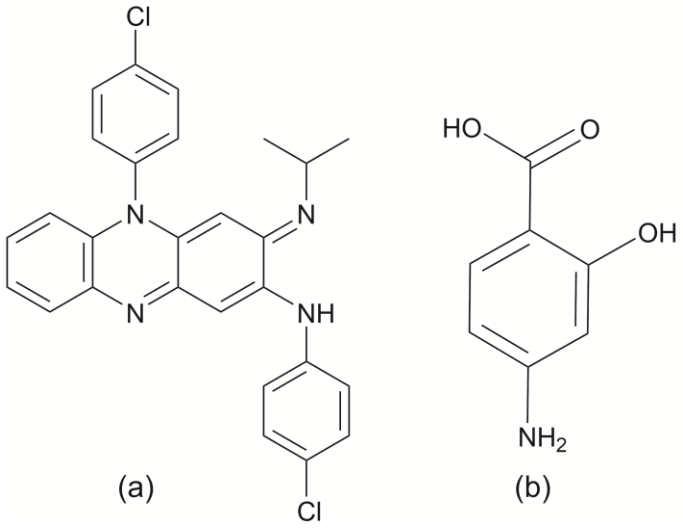

Figure 1. Molecular diagram of (a) clofazimine (CFZ) and (b) 4-aminosalicylic acid (PAS).

TGA/DSC

Thermal stability of the four forms was evaluated with a TGA/DSC3+ apparatus (Mettler Toledo). Solid samples were analysed in open aluminium pans (100 µL) from 25 to 300°C (at a 10 °C/min scanning rate) under a nitrogen flow (80 mL/min). Results were analyzed with the STARe software (version 16.20).

Water solubility evaluation

Solubility of CFZ, PAS and CFZNH$^+$-PAS$^-$ salt (forms I to IV) was evaluated in type I water, by wetting an excess amount of powder (10-20 mg) in 2.0 mL type I water at 25°C (Heidolf incubator 1000) and under agitation at 900 rpm (Heidolf titramax 1000 platform shaker). Experiments were performed in triplicate. After 24 hours, the samples were centrifuged at 13000 rpm (eppendorf centrifuge 5430R, equipped with a FA-45-24-11 rotor) for 15 minutes, the supernatant was recovered and centrifuged again (15 minutes, 13000 rpm). After second centrifugation, the supernatant was diluted twice with MeCN. Solubility was evaluated by an HPLC method performed with a Zorbax SB C18 (3.5 µm, 3 x 100 mm) column heated to 40°C and connected on an Agilent 1100 series HPLC system using UV detection at 280 and 490 nm. Gradient elution was performed with mobile phase A (trifluoroacetic acid 0.1%) and mobile phase B (MeCN) at a flow rate of 0.5 mL/min. Gradient started at 15% B and ramped up to 70% B in 0.5 minute. This solvent ratio was maintained for 6.5 minutes before returning to 15% B for 6 minutes to re-equilibrate the column. The injection volume was 5 µL. Calibration was performed with samples prepared in MeCN/water 1:1 (in volume) with concentrations ranging from 16.6 to 0.06 µg/mL for CFZ and from 80 to 1.25 µg/mL for PAS. pH of the salt solutions (forms I, II, III and IV) was measured after first centrifugation and, in all cases, it was comprised between 4.5 and 4.9.

Stability in Fasted-state simulated gastric fluid (FaSSGF)

Propensity of CFZNH$^+$-PAS$^-$ to undergo anion exchange in gastric fluid was evaluated by dispersing an excess amount of each form in FaSSGF. After 30 minutes, the PXRD pattern of the remaining solid was collected with a STOE MP diffractometer. Fasted-state simulated gastric fluid was prepared by solubilisation of 0.0597 g of FaSSIF/FeSSIF/FaSSGF powder in 1.0 L of a NaCl (1.999 g/L) solution adjusted with HCl at pH 1.6.

Relative stability of the four forms

Relative stability of the four forms was evaluated by competitive slurry experiments in water at 22°C. Mixtures of two forms (I and II, I and III, I and IV, II and III, II and IV and III and IV) were suspended in water for 14 days. The solid phase was then recovered and analyzed in PXRD.

Evaluation of CFZNH$^+$-PAS$^-$ salts hygroscopicity

Dynamic vapour sorption (DVS) analyses were performed on a Q5000 SA apparatus (TA instruments) at 25°C with nitrogen as flow gas (50 mL/min). Solid samples (7-15 mg) were placed in platinum crucible (empty crucible used as a reference) and inserted in a temperature and humidity controlled chamber. Samples were first dried at 40°C for 1 hour and then exposed to variable relative humidity (10 to 90%) at 25°C. Equilibrium was considered to be reached when no weight change is observed for two hours of exposure or if it is less than 0.010 mg/min.

Results

Forms I to III of CFZNH$^+$-PAS$^-$ salt were prepared by liquid-assisted grinding. PXRD patterns of the ground powders were compared to the one of the starting materials and in each case a new crystalline phase was identified (Fig. 2).

Single-crystals were obtained for form I (data were collected at 295 K and 100 K) and for a solvated salt (CFZNH$^+$-PAS$^-$-MeCN (1:1:1), data collected at 100 K). Structure of form II was determined from powder data. Both forms (I and II) crystallize in $P\bar{1}$ triclinic space group and their asymmetric units contain one clofaziminium cation (CFZNH$^+$) and one 4-aminosalicylate anion (PAS$^-$) (Table S1).

Form III was first identified during competitive slurry of forms I and II in water and could be successfully obtained by liquid-assisted grinding of clofazimine with 4-aminosalicylic acid in presence of EtOAc. Form IV was first identified after solubility evaluation of form I and could be obtained by slurrying clofazimine and 4-aminosalicylic acid

in water (Fig. 2). Despite several attempts, up to now, structures of forms III and IV could not be determined.

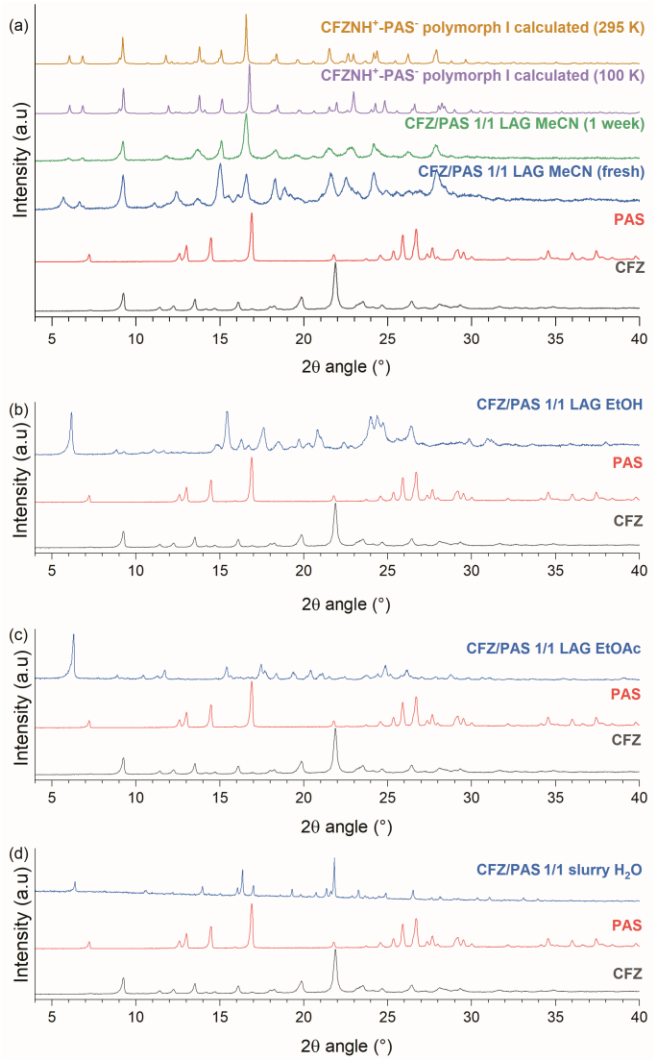

Figure 2. PXRD pattern of, from bottom to top: CFZ, PAS and (a) CFZ/PAS 1/1 LAG MeCN and calculated pattern of $CFZNH^+$-PAS^- form I at 100K and 295K, (b) CFZ/PAS 1/1 LAG EtOH (form II), (c) CFZ/PAS 1/1 LAG EtOAc (form III) and (d) CFZ/PAS 1/1 slurry H_2O (form IV).

Polymorph I

Crystals were dried at room temperature before SCXRD data collection. PAS^- is disordered over 3 positions with respective occupancy (at 100K) of 0.493, 0.199 and 0.307 (disorder identified by letters A, B and C in atom labelling). Strong charge-assisted hydrogen bonds are observed between $CFZNH^+$ cation and PAS^- anion ($N4^+$-H···$O1A^-$, N3-H···$O1A^-$, Fig. 3a and Table S2). Other H-bond interactions are presented in Table S2.

Clofaziminium cations are stacked in a head to tail fashion (centroid-centroid distance of 3.672(2) Å, orthogonal projection distance of 3.519(1) Å and horizontal displacement of 1.046 Å, Fig. 3b). C-H···π interactions are further observed between $CFZNH^+$ cation and PAS^- anion (H26C···centroid distance of 2.68 Å, orthogonal projection distance of 2.68 Å, C26···centroid distance of 3.643(9) Å and C26-H26C···π angle of 78 °, Fig. 3 c). Interestingly powder obtained just after LAG in presence of MeCN does not correspond to $CFZNH^+$-PAS^- form I. This phase is however unstable at room temperature and spontaneously converts to form I as indicated by PXRD pattern measured on freshly prepared powder and after one week of storage at room temperature (Fig. 2).

Polymorph II

$CFZNH^+$ and PAS^- interact through charge-assisted H-bonds ($N4^+$-H···$O1A^-$, N3-H···$O1A^-$, Fig. 3d) and Table S2). Clofaziminium cations are stacked in a head to tail fashion (centroid-centroid distance of 3.760(16) Å, orthogonal projection distance of 3.682(13) Å and horizontal displacement of 0.767 Å, Fig. 3e). Two C-H···π interactions are observed between $CFZNH^+$ cation and PAS^- anion (H26B···centroid distance of 2.95(9) Å, orthogonal projection distance of 2.81 Å, C26···centroid distance of 3.85(8) Å and C26-H26B···π angle of 78 ° as well as H4···centroid distance of 2.63(8) Å, orthogonal projection distance of 2.44 Å, C4···centroid distance of 3.48(8) Å and C4-H4···π angle of 84 °, Fig. 3f). Structure of this second form of $CFZNH^+$-PAS^- was determined from PXRD data collected on a powder of CFZ/PAS 1/1 LAG EtOH (Table S1). Observed, calculated and difference patterns are shown in supplementary information (Fig. S1).

Thermal analysis

TG/DSC analysis performed on a freshly prepared powder of CFZ/PAS 1/1 LAG MeCN (Fig 4a) suggests that this phase is solvated as a weight loss (associated with a wide endotherm on the DSC curve (onset 51°C)) is observed from 25°C to around 95°C. This assumption has been confirmed by the determination of the crystal structure of $CFZNH^+$-PAS^--MeCN (1:1:1) solvate (Fig. S2 and Tables S1 and S2). A small exothermic event, not associated with any weight loss, is observed at 129°C and, at 215°C, melting occurs, immediately followed by degradation (probably associated with PAS decarboxylation).

A variable-temperature PXRD experiment performed on freshly prepared powder of CFZ/PAS 1/1 LAG MeCN indicates the formation of $CFZNH^+$-PAS^- form I upon heating (Fig. S3). Then, between 130 and 150°C, a transformation occurs. Actually, a partial conversion of form I to form II is observed upon heating. A kinetically controlled process is suspected for this conversion and exact condition of conversion could not be determined (Figs. S3 and S4).

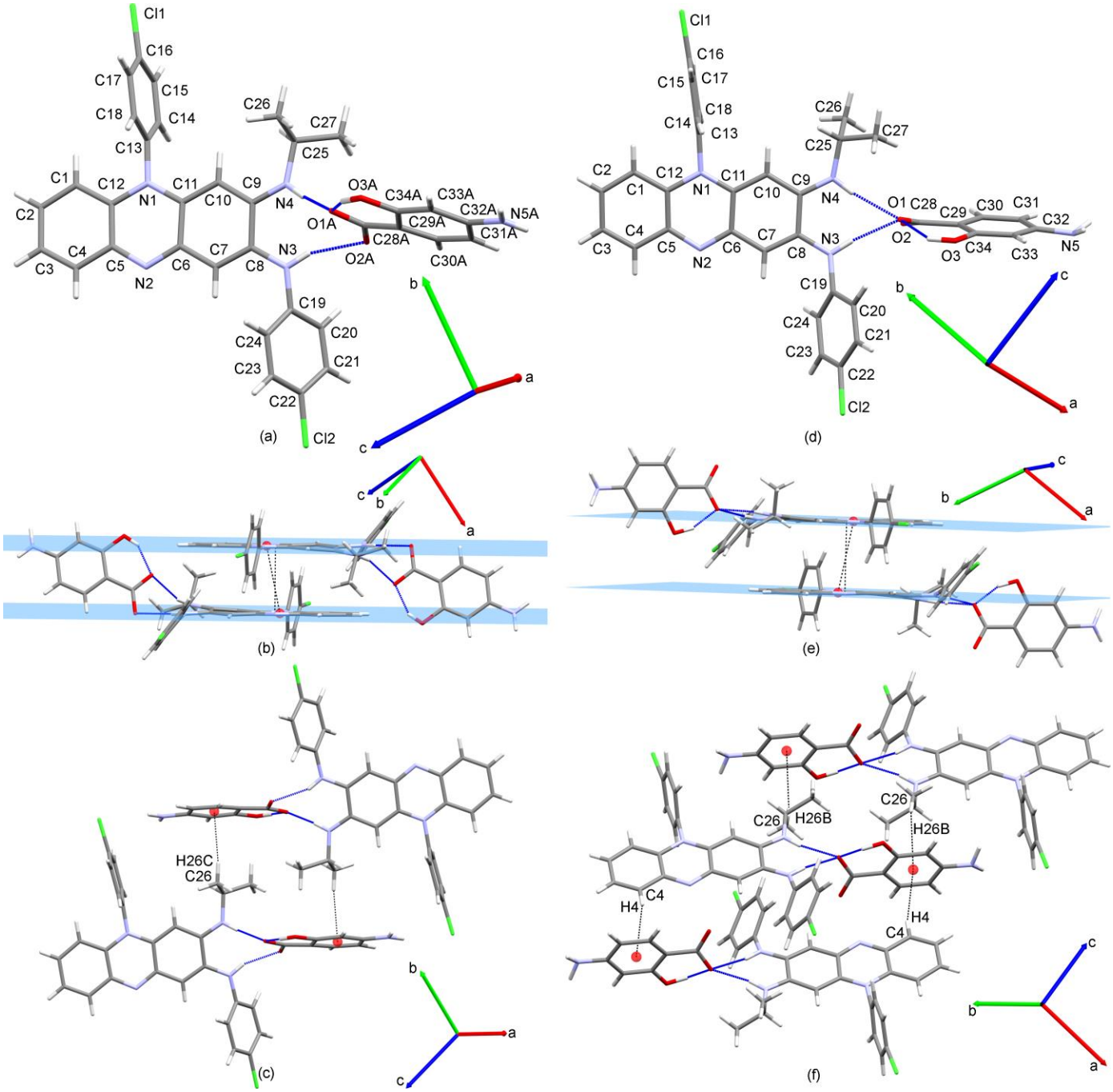

Figure 3. Crystal structures of $CFZNH^{+}$-PAS^{-} forms I (left) and II (right). Asymmetric unit and labelling (top), stacking of $CFZNH^{+}$ cations (centroids (red) and planes (blue) calculated with C5, C6, N1, N2, C11 and C12 atoms) (middle) and C-H···π interaction between $CFZNH^{+}$ and PAS^{-} (centroids calculated with C29, C30, C31, C32, C33 and C34 atoms (position A of PAS considered in form I) (bottom).

A new TG/DSC analysis (Fig. 4b) performed on powder corresponding to form I (CFZ/PAS LAG MeCN after one week of storage at room temperature) does not present any weight loss between 25 and 95°C confirming complete

phase transformation from a solvate to form I in these conditions. A small exothermic event is observed at 126°C (consistent with phase transformations identified by variable temperature PXRD) before melting and degradation at 217°C.

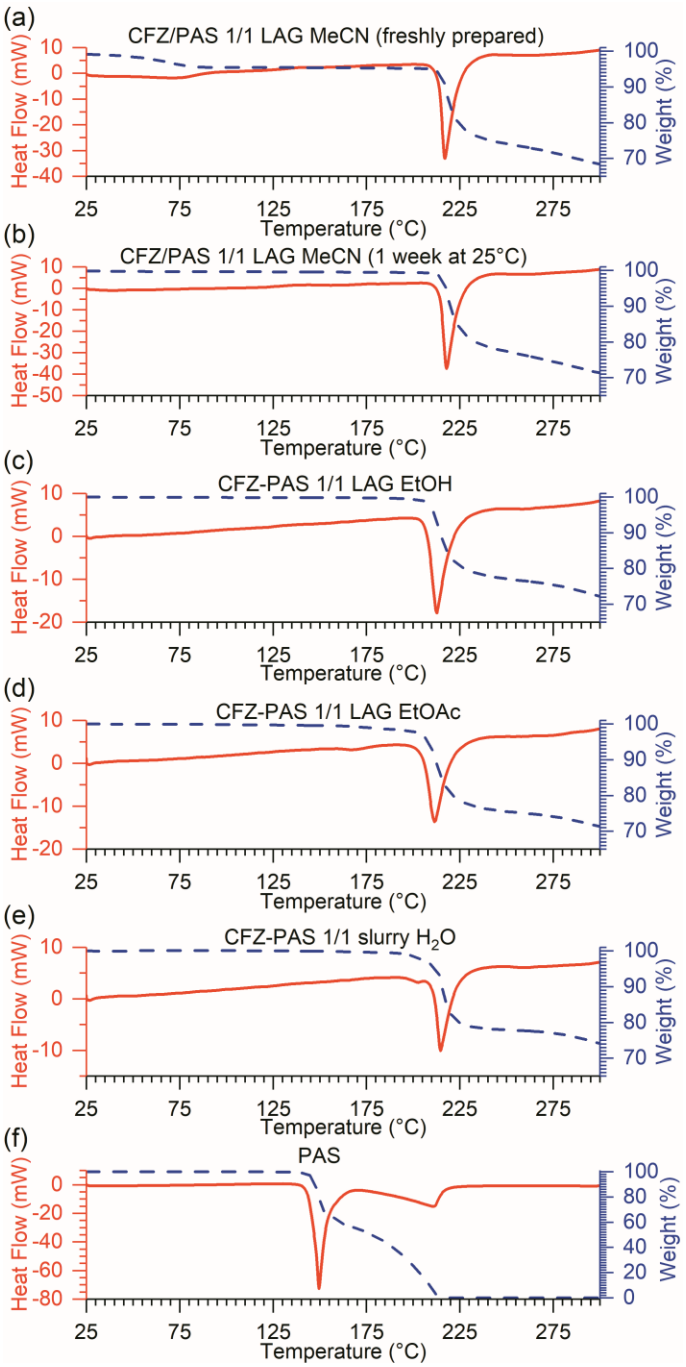

Figure 4. TGA (dashed blue) and DSC (plain red) curves of (a) CFZ/PAS 1/1 LAG MeCN (powder freshly prepared), (b) $CFZNH^+$-PAS^- form I, (c) $CFZNH^+$-PAS^- form II, (d) CFZ/PAS 1/1 LAG EtOAc (form III), (e) CFZ/PAS 1/1 slurry H_2O (form IV) and (f) PAS.

In Fig. 4c, thermal stability of form II was evaluated by TGA/DSC. Results indicated that this form is stable up to 210°C, temperature at which melting and degradation occur.

Thermal analysis of form III (Fig. 4d) reveals an endothermic event (162°C), corresponding to a phase conversion from form III to form II (Figure S5), before melting and degradation at 209°C.

TG/DSC analysis of form IV reveals the presence of a small endotherm at 202°C (associated to a 4% weight loss). This event is followed by a second endotherm associated to melting and further degradation of the phase at 214°C.

$CFZNH^+$-PAS^- behaviour in solution

Solubility of CFZ, PAS, $CFZNH^+$-PAS^- (forms I to IV) was studied in water at 25°C by an HPLC method. Results indicate that after 24h of dispersion in water, only 0.20 ± 0.03 µg/mL of clofazimine is released in solution (Fig. 5).

PAS solubility could not be determined because PAS degrades in water (two peaks are observed on the chromatogram (Fig. S6)). Such degradation is not observed for $CFZNH^+$-PAS^- salts (forms I to IV).

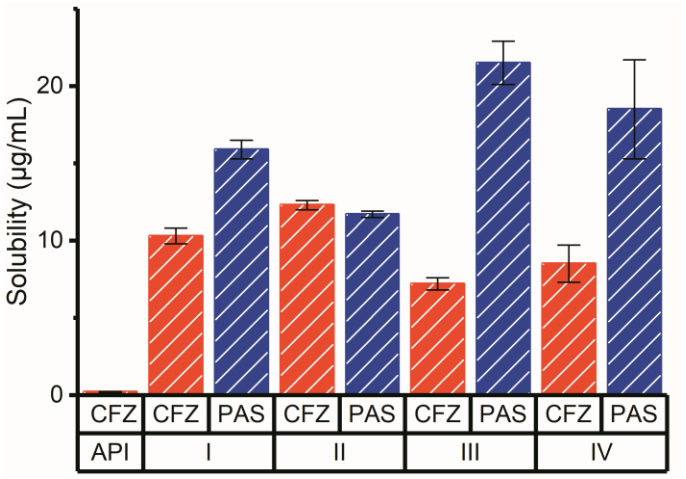

Figure 5. Amount of CFZ (red) and PAS (blue) released after 24h in water from CFZ and the four salts (forms I to IV).

All four forms present a significant increase of CFZ solubility after 24h in water (Fig.5). Indeed, the amount of solubilized CFZ reaches 10.26 ± 0.52 µg/mL (50-fold improvement), 12.27 ± 0.32 µg/mL (60-fold solubility improvement), 7.15 ± 0.43 µg/mL (36-fold improvement) and 8.50 ± 1.24 µg/mL (42-fold improvement) from $CFZNH^+$-PAS^- forms I to IV respectively. The amount of solubilized PAS is 15.94 ± 0.55 µg/mL, 11.70 ± 0.17 µg/mL, 21.47 ± 1.37 µg/mL and 18.47 ± 3.15 µg/mL from forms I to IV respectively.

PXRD analysis of the remaining powder (after 24h dispersion in water) indicates that CFZ does not undergo any crystalline phase change, $CFZNH^+$-PAS^- forms II, III and IV remain stable in water for 24h, while form I converts to a mixture of form III and form IV. PAS degradation is not observed on PXRD pattern collected after solubility evaluation of PAS (Fig.6a). This could be explained by the high aqueous solubility (26.29 g/L at 20°C[6]) of the PAS degradation product, 3-aminophenol, in water.

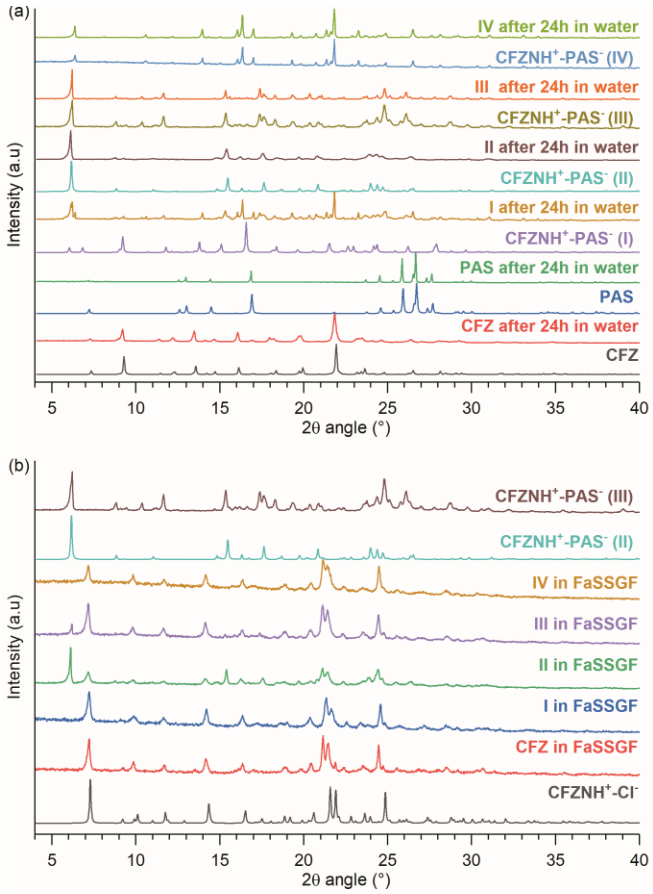

Figure 6. PXRD patterns, (a) of CFZ, PAS, $CFZNH^+$-PAS^- forms I, II, III and IV before and after dispersion in water and (b) of $CFZNH^+$-Cl^- (calculated pattern), CFZ, $CFZNH^+$-PAS^- (forms I to IV) after dispersion in FaSSGF, and powder patterns of $CFZNH^+$-PAS^- (II, calculated) and of form III.

Bannigan *et al*.[16] reported anion exchange and $CFZNH^+Cl^-$ precipitation after dispersion of CFZ salts in simulated gastric fluids. The propensity of $CFZNH^+$-PAS^- for anion exchange was investigated by a slurry experiment of all four forms in FaSSGF. Powders recovered after dispersion of form I or IV correspond to $CFZNH^+Cl^-$, while the ones recovered after dispersion of form II or III in FaSSGF correspond to a mixture of $CFZNH^+Cl^-$ with $CFZNH^+$-PAS^- (form II or III respectively) (Fig. 6b). Those data are consistent with what is reported in literature[16] and indicate rapid anion exchange and precipitation of the hydrochloride salt of clofazimine.

Relative stability of the four forms

Competitive slurry experiments of forms I and II, of forms I and III as well as of forms II and III lead to form III (Fig. 7). This indicates that both forms I and II are less stable than form III in water. Relative stability of forms I and II could not be determined as both are metastable (conversion to form III is already achieved after 48h). All competitive slurry experiments implying form IV lead to form IV indicating that this is the most stable one in water (Fig. 7). The relative stability in water at 22°C can thus be established as $CFZNH^+$-PAS^- (I), $CFZNH^+$-PAS^- (II) < $CFZNH^+$-PAS^- (III) < $CFZNH^+$-PAS^- (IV).

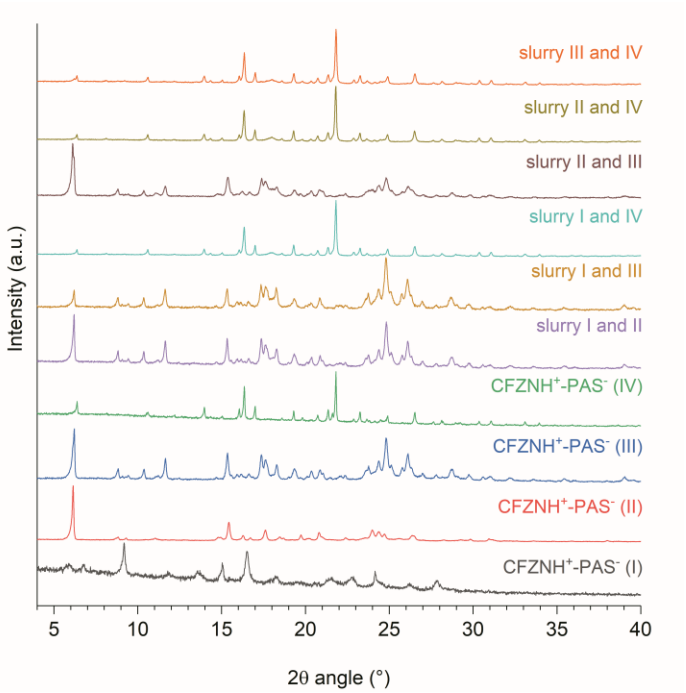

Figure 7. PXRD patterns of the solid phases recovered after 14 days of competitive slurry experiments of forms I and II, forms I and III, forms I and IV, forms II and III, forms II and IV and of forms III and IV compared to the powder patterns of forms I, II, III and IV.

Evaluation of $CFZNH^+$-PAS^- salts water sorption

Dynamic vapour sorption analyses were performed on the four forms identified. No deliquescence or significant water uptake was observed (Fig. 8) except for form I that reversibly absorbs around 3% water at 90% humidity (Fig. 8a). Such a 3% water absorption may correspond to a monohydrated (calculated water content of 2.8%) form of the salt. Besides, the isotherm hysteresis (Fig. 8a)

evidences the existence of a hydrated form of CFZNH$^+$-PAS$^-$ (I).

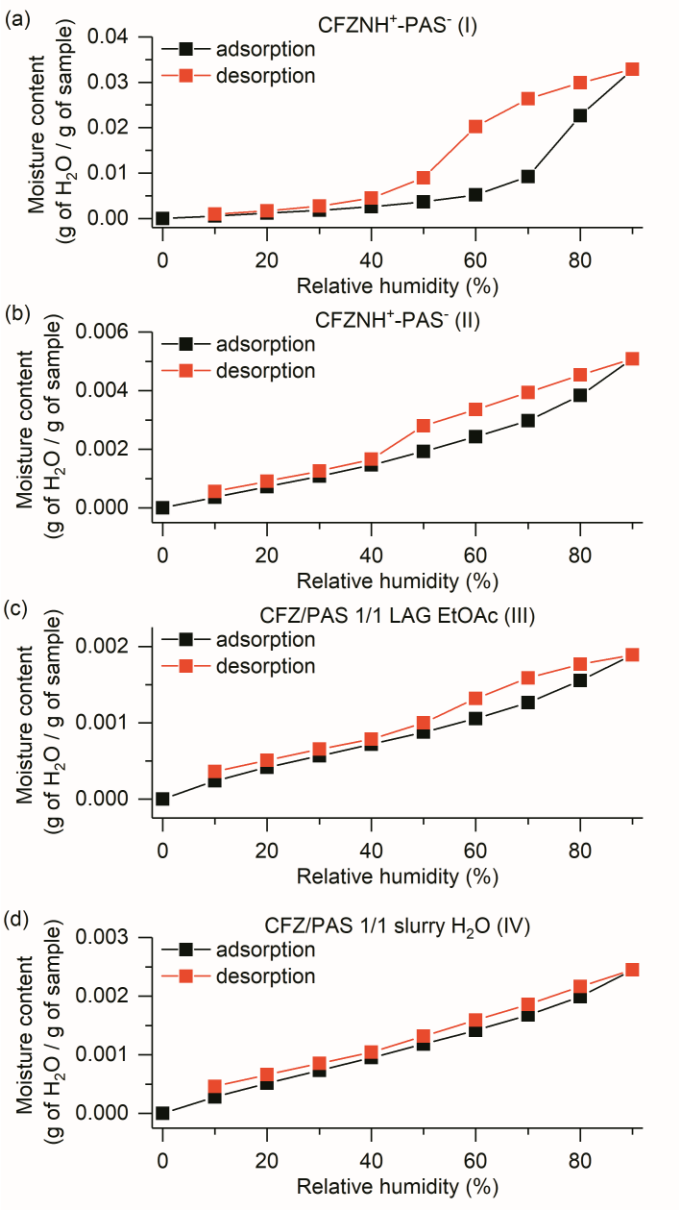

Figure 8. Sorption isotherms (adsorption and desorption) of CFZNH$^+$-PAS$^-$ form I (a), form II (b), form III (c) and form IV(d).

Discussion

Thermal analyses of the four identified forms indicate that form I undergo a phase conversion (between 120 and 150°C), followed by melting at 215°C. Form III converts to form II, which melts at 209°C, upon heating. Thermal behaviour of form IV is more complicated as a small endotherm associated to a 4% weight loss is observed at 202°C before melting at 214°C. A 2.9% weight loss would be expected for a monohydrate, however the high temperature at which the 4% weight loss is observed suggests that this phase does not correspond to an hydrated form of a clofaziminium 4-aminosalicylate salt.

For all forms identified, melting is immediately followed by degradation, most probably through decarboxylation of PAS. CFZNH$^+$-PAS$^-$ salts present an increased thermal stability in comparison to pure PAS (which decarboxylates at 145°C). Decarboxylation of pure PAS can however occur at lower temperature but with longer induction period (59 hours at 74°C, 12.2 hours at 78°C, 5 hours at 90°C[23]). The increased thermal stability observed for all the four forms could probably be attributed to the presence of strong interactions (charged-assisted H-bonds, as observed in the structures of polymorphs I and II) between clofaziminium and the carboxylate of PAS. These interactions would probably prevent CO_2 release from PAS before melting of the salt. Such kind of interaction between clofaziminium and carboxylate was already reported in several studies[15,17,40]. More particularly improved solubility was observed for a clofaziminium mesylate salt presenting the same type of interaction[15]. Furthermore, such kind of strong interaction was also shown to improve physical stability of amorphous solid dispersion of clofazimine and hypromellose phthalate[40].

Pure PAS also decarboxylates in water, however decarboxylation of its sodium salt occurs to a lesser extent in water thanks to the higher pH of the PAS·Na solution in comparison to the PAS solution. We believe that the preparation of CFZNH$^+$-PAS$^-$ could potentially have a similar effect and that it could be beneficial for compound storage (moisture accelerates PAS decarboxylation and higher pH could slower the reaction). This hypothesis is supported by the absence of PAS degradation peak on the HPLC chromatograms measured after a 24h dispersion of CFZNH$^+$-PAS$^-$ salts in water.

Solubility study performed in water indicates a significant increase of solubilized CFZ (10.26 ± 0.52 µg/mL (form I), 12.27 ± 0.32 µg/mL (form II), 7.15 ± 0.43 µg/mL (form III) and 8.50 ± 1.24 µg/mL (form IV)) from CFZNH$^+$-PAS$^-$ salts in comparison to pure CFZ (0.20 ± 0.03 µg/mL). Interestingly, forms III and IV have very similar solubility in water (same value within experimental errors). Furthermore, CFZNH$^+$-PAS$^-$ salt preparation prevents PAS decarboxylation in water as indicated by the absence of degradation peak on the HPLC chromatogram.

Slurry of all four forms in FaSSGF has shown anion exchange and formation of CFZNH$^+$Cl$^-$. In consequence, CFZ bioavailability could be reduced because of the formation of CFZNH$^+$Cl$^-$ in the stomach. Preparation of gastro-resistant caps of CFZNH$^+$-PAS$^-$ could be an alternative, among others, that could potentially avoid or

reduce PAS decarboxylation and $CFZNH^+Cl^-$ formation in the stomach while maintaining an improved solubility profile for $CFZNH^+$-PAS^-.

Competitive slurry experiments performed at 22°C in water have shown both the forms I and II are less stable than form III which is in accordance with the fact that the latter is less soluble than forms I and II in water. The most stable form in these conditions is form IV.

DVS analyses have shown that none of the four presented forms is deliquescent. A reversible 3% water sorption is however observed for form I, which could correspond to the formation of a monohydrated form. Water desorption suggests however that this potential hydrated form is not stable at low relative humidity. For all the other forms, measured water sorption is less than 1% even at 90% relative humidity exposure.

Conclusion

Four forms of a salt combining clofazimine and 4-aminosalicylic acid, two antitubercular drugs susceptible to be co-administered in patients suffering from XDR-TB, were identified by liquid-assisted grinding. Forms I and II have been structurally described and their thermal properties have been investigated by TGA/DSC. Two other forms for which structure could not be determined were also discovered. The preparation of these four forms resulted in an improved thermal stability towards PAS decarboxylation in comparison to pure PAS. This stabilization is also observed in water and it can probably be attributed to weak basicity of CFZ which increases pH of the solution and thus slows down the PAS decarboxylation.

Preparation of $CFZNH^+$-PAS^- salt resulted in an important increase of solubilized CFZ (50-fold and 60-fold CFZ solubility improvement from $CFZNH^+$-PAS^- forms I and II and around 40-fold improvement from forms III and IV which have same solubility within experimental errors). During the solubility test of $CFZNH^+$-PAS^- form I, a phase transformation in water has been observed with this polymorphic form while no phase transformation is observed during solubility evaluation for the three other forms.

Competitive slurry experiments have shown that form IV is the most stable one in water at 22°C. Form II is more soluble than forms III and IV but the latter two are more stable in water.

DVS analyses have shown a 3% water sorption at 90% relative humidity exposure for form I. The three other forms present a good stability regarding hygroscopicity as no significant water sorption is observed during DVS analyses.

The phase transformation and the reversible water sorption observed for form I suggest that this phase could be more challenging for further development. The three other forms (II, III and IV) are interesting for further investigation but care has to be taken regarding phase transformation as several forms of $CFZNH^+$-PAS^- salts were identified.

If such combinations of CFZ with PAS could lead to improved bioavailability *in vivo* remains to be determined. A gastro-resistant formulation of $CFZNH^+$-PAS^- would probably be necessary in order to avoid PAS decarboxylation and $CFZNH^+Cl^-$ precipitation in the stomach. However, the present study suggests that salification of CFZ (BCS II) with PAS (BCS III drug) could lead to improved physico-chemical properties of both parent APIs.

Conflict of interest: There is no conflict to declare.

Acknowledgement: L.B. thanks the FRS-FNRS for the funding (research fellow grant) and Lionel Pochet for his help for the elaboration of the HPLC method. X. B. thanks the Fonds Européen de Développement Régional, European Union and the “Walloon Region” for their financial support in the operational framework Wallonie2020.EU. This work was performed on XRD and TA equipments from the PC2 platform at the University of Namur.This research used resources of the "Plateforme Technologique de Calcul Intensif (PTCI)" (http://www.ptci.unamur.be) located at the University of Namur, Belgium, which is supported by the FNRS-FRFC, the Walloon Region, and the University of Namur (Conventions No. 2.5020.11, GEQ U.G006.15, 1610468, and RW/GEQ2016). The PTCI is member of the "Consortium des Équipements de Calcul Intensif (CÉCI)" (http://www.cecihpc.be).

References

1. World Health Organization. *Global Tuberculosis Report 2019.* Geneva: World Health Organization; 2019.

2. World Health Organization. *Guidelines for Treatment of Drug-Susceptible Tuberculosis and Patient Care*. (World Health Organization, ed.). Geneva: World Health Organization; 2017.

3. Sotgiu G, Tiberi S, Centis R, et al. International Journal of Infectious Diseases Applicability of the shorter “ Bangladesh regimen ” in high multidrug-resistant tuberculosis settings §. *Int J Infect Dis*. 2017;56:190-193. doi:10.1016/j.ijid.2016.10.021.

4. Lange C, Chesov D, Heyckendorf J. Clofazimine for the treatment of multidrug-resistant tuberculosis. *Clin Microbiol Infect*. 2019;25(2):128-

130. doi:10.1016/j.cmi.2018.11.010.

5. World Health Organization. *WHO Consolidated Guidelines on Drug-Resistant Tuberculosis Treatment*.; 2019. https://www.who.int/tb/publications/2019/consolidated-guidelines-drug-resistant-TB-treatment/en/.

6. Yalkowsky SH, He Y, Jain P. *Handbook of Aqueous Solubility Data*. CRC press; 2016.

7. Bevan CD, Lloyd RS. A high-throughput screening method for the determination of aqueous drug solubility using laser nephelometry in microtiter plates. *Anal Chem*. 2000;72(8):1781-1787.

8. Schwinté P, Ramphul M, Darcy R, O'sullivan JF. Amphiphilic cyclodextrin complexation of clofazimine. *J Incl Phenom Macrocycl Chem*. 2003;47(3-4):109-112.

9. Salem II, Steffan G, Düzgünes N. Efficacy of clofazimine-modified cyclodextrin against Mycobacterium avium complex in human macrophages. *Int J Pharm*. 2003;260(1):105-114. doi:10.1016/S0378-5173(03)00236-9.

10. Li S, Chan JY-W, Li Y, et al. Complexation of clofazimine by macrocyclic cucurbit [7] uril reduced its cardiotoxicity without affecting the antimycobacterial efficacy. *Org Biomol Chem*. 2016;14(31):7563-7569.

11. Zhang Y, Feng J, McManus SA, et al. Design and solidification of fast-releasing clofazimine nanoparticles for treatment of cryptosporidiosis. *Mol Pharm*. 2017;14(10):3480-3488.

12. Patel VR, Agrawal YK. Nanosuspension: An approach to enhance solubility of drugs. *J Adv Pharm Technol Res*. 2011;2(2):81.

13. Narang AS, Srivastava AK. Evaluation of solid dispersions of clofazimine. *Drug Dev Ind Pharm*. 2002;28(8):1001-1013. doi:10.1081/DDC-120006431.

14. O'Reilly JR, Corrigan OI, O'Driscoll CM. The effect of simple micellar systems on the solubility and intestinal absorption of clofazimine (B663) in the anaesthetised rat. *Int J Pharm*. 1994;105(2):137-146. doi:10.1016/0378-5173(94)90459-6.

15. Bolla G, Nangia A. Clofazimine mesylate: A high solubility stable salt. *Cryst Growth Des*. 2012;12(12):6250-6259. doi:10.1021/cg301463z.

16. Bannigan P, Durack E, Madden C, Lusi M, Hudson SP. Role of Biorelevant Dissolution Media in the Selection of Optimal Salt Forms of Oral Drugs: Maximizing the Gastrointestinal Solubility and in Vitro Activity of the Antimicrobial Molecule, Clofazimine. *ACS Omega*. 2017;2(12):8969-8981. doi:10.1021/acsomega.7b01454.

17. Bodart L, Tumanov N, Wouters J. Structural variety of clofaziminium salts: effect of the counter-ion on clofaziminium conformation and crystal packing. *Acta Crystallogr Sect B Struct Sci Cryst Eng Mater*. 2019;75(4).

18. Sousa ML, Sarraguça MC, dos Santos AO, Sarraguça JMG, Lopes J, da Silva Ribeiro PR. A new salt of clofazimine to improve leprosy treatment. *J Mol Struct*. 2020:128226.

19. Zheng J, Rubin EJ, Bifani P, et al. para-Aminosalicylic acid is a prodrug targeting dihydrofolate reductase in Mycobacterium tuberculosis. *J Biol Chem*. 2013;288(32):23447-23456.

20. del Moral-Sanchez J-M, Gonzalez-Alvarez I, Gonzalez-Alvarez M, Navarro A, Bermejo M, others. Classification of WHO Essential Oral Medicines for Children Applying a Provisional Pediatric Biopharmaceutics Classification System. *Pharmaceutics*. 2019;11(11):567.

21. Rekker RF, Nauta WT. The UV Absorption Spectra of p-Aminosalicylic Acid and some Related Compounds--IV. The Ampholytic Forms of p-Aminosalicylic Aicd and some Structurally Related Compounds and their Decarboxylation. *J Med Chem*. 1959;2(3):281-297.

22. Kornblum SS, Sciarrone BJ. Decarboxylation of p-aminosalicylic acid in the solid state. *J Pharm Sci*. 1964;53(8):935-941.

23. Rotich M, Glass B, Brown M. Thermal studies on some substituted aminobenzoic acids. *J Therm Anal Calorim*. 2001;64(2):681-688.

24. Wesolowski M. The decarboxylation and thermal stability of p-amino-salicylic acid and its salts. *Thermochim Acta*. 1977;21(2):243-253.

25. Way EL, Smith PK, Howie DL, Weiss R, Swanson R. The absorption, distribution, excretion and fate of para-aminosalicylic acid. *J Pharmacol Exp Ther*. 1948;93(3):368-382.

26. European Medicines Agency, EMA. *Assessment Report Para-Aminosalicylic Acid Lucane*.; 2014.

27. World Health Organization. *Companion Handbook to the WHO Guidelines for the Programmatic Management of Drug-Resistant Tuberculosis*.

World Health Organization; 2014.

28. Xu H-B, Jiang R-H, Xiao H-P. Clofazimine in the treatment of multidrug-resistant tuberculosis. *Clin Microbiol Infect*. 2012;18(11):1104-1110.

29. Zhang S, Shi W, Feng J, Zhang W, Zhang Y. Varying effects of common tuberculosis drugs on enhancing clofazimine activity in vitro. *Emerg Microbes Infect*. 2017;6(4):e28.

30. Lu Y, Wang B, Zhao WJ, et al. A study on the activity of clofazimine with antituberculous drugs against Mycobacterium tuberculosis. *Chinese J Tuberc Respir Dis*. 2010;33(9):675-678.

31. Clark RC, Reid JS. The Analytical Calculation of Absorption in Multifaceted Crystals. *Acta Crystallogr A*. 1995;51:887-897. doi:10.1107/S0108767395007367.

32. Rigaku Oxford Diffraction. CrysAlis PRO. Version 1.171.40.67a. *CrysAlis PRO*. 2019:Rigaku Oxford Diffraction Ltd, Yarnton, England.

33. Sheldrick GM. SHELXT - Integrated space-group and crystal-structure determination. *Acta Crystallogr Sect A Found Crystallogr*. 2015;71(1):3-8. doi:10.1107/S2053273314026370.

34. Dolomanov O V., Bourhis LJ, Gildea RJ, Howard JAK, Puschmann H. OLEX2: A complete structure solution, refinement and analysis program. *J Appl Crystallogr*. 2009;42(2):339-341. doi:10.1107/S0021889808042726.

35. Sheldrick GM. Crystal structure refinement with SHELXL. *Acta Crystallogr Sect C Struct Chem*. 2015;71:3-8. doi:10.1107/S2053229614024218.

36. Hübschle CB, Sheldrick GM, Dittrich B. ShelXle : a Qt graphical user interface for SHELXL. *J Appl Crystallogr*. 2011;44:1281-1284. doi:10.1107/S0021889811043202.

37. Macrae CF, Sovago I, Cottrell SJ, et al. Mercury 4.0: from visualization to analysis, design and prediction. *J Appl Crystallogr*. 2020.

38. Favre-Nicolin V, Radovan C. FOX , ` free objects for crystallography ': a modular approach to ab initio structure determination from powder diffraction. *J Appl Crystallogr*. 2002;35:734-743. doi:10.1107/S0021889802015236.

39. Coelho AA. TOPAS and TOPAS-Academic : an optimization program integrating computer algebra and crystallographic objects written in C ++. *J Appl Crystallogr*. 2018;51:210-218. doi:10.1107/S1600576718000183.

40. Nie H, Su Y, Zhang M, et al. Solid-state spectroscopic investigation of molecular interactions between clofazimine and hypromellose phthalate in amorphous solid dispersions. *Mol Pharm*. 2016;13(11):3964-3975.